



HAL
open science

High resolution seismic tomography of a Strombolian volcanic cone

F. Brenguier, Olivier Coutant, H. Baudon, M. Dietrich

► **To cite this version:**

F. Brenguier, Olivier Coutant, H. Baudon, M. Dietrich. High resolution seismic tomography of a Strombolian volcanic cone. *Geophysical Research Letters*, 2006, VOL. 33, pp.L16314. 10.1029/2006GL026902 . insu-00265578

HAL Id: insu-00265578

<https://insu.hal.science/insu-00265578>

Submitted on 12 Mar 2021

HAL is a multi-disciplinary open access archive for the deposit and dissemination of scientific research documents, whether they are published or not. The documents may come from teaching and research institutions in France or abroad, or from public or private research centers.

L'archive ouverte pluridisciplinaire **HAL**, est destinée au dépôt et à la diffusion de documents scientifiques de niveau recherche, publiés ou non, émanant des établissements d'enseignement et de recherche français ou étrangers, des laboratoires publics ou privés.

High resolution seismic tomography of a Strombolian volcanic cone

F. Brenguier,¹ O. Coutant,¹ H. Baudon,¹ F. Doré,¹ and M. Dietrich¹

Received 15 May 2006; revised 28 June 2006; accepted 13 July 2006; published 26 August 2006.

[1] We determine the 3D velocity structure of the Puy des Goules, a small, 1 km wide, Strombolian volcano that erupted 10 ky ago in central France, through a high resolution seismic survey. One major goal for this experiment was to develop methods to reach a high resolution focused on the plumbing system. This has raised different problems such as: mixing active sources (explosive, vibroseis) with different signal properties; inverting traveltimes residuals of the order of 10 ms which requires the corresponding accuracy on the Digital Elevation Model (DEM), source and sensor locations (300 sites) and traveltimes computations. The results of the traveltimes tomography reveal three main bodies of high velocity embedded within scoria layers. These bodies can be interpreted as the central chimney and two complex feeding zones that compare quite well with the Puy de Lemptégy, a neighboring cone that was quarried and removed, showing its underlying feeding conduits and dykes. These results represent a first step toward our objective that is to determine geological structures related to natural hazards with a high resolution. **Citation:** Brenguier, F., O. Coutant, H. Baudon, F. Doré, and M. Dietrich (2006), High resolution seismic tomography of a Strombolian volcanic cone, *Geophys. Res. Lett.*, 33, L16314, doi:10.1029/2006GL026902.

1. Introduction

[2] In the last decade, seismic tomographies on volcanoes have provided structure images with an increasing resolution [e.g., *Laigle et al.*, 2000; *Zollo et al.*, 2002; *Tanaka et al.*, 2002; *Yamawaki et al.*, 2004]. For most of these studies, the objective is to determine the velocity structure of the entire volcano, or to map details such as possible location of melt material, shallow magma reservoir, or heterogeneities that correlate with seismic activity [*Kodaira et al.*, 2002]. These experiments have an horizontal extent of 10 to 20 km, a depth of investigation of a few kilometers, and a spatial resolution of the order of 1 km (less for *Scarpa et al.* [2002]). One challenge for seismic tomography on volcanoes however, is to resolve much finer details and to provide images of metric to decametric structures such as the plumbing system, or zones with mechanical weakness leading to flank collapse. To obtain a decametric resolution over a distance of 10 km requires recording densities as high as those used in marine exploration. This is obviously out of reach on land and in rough field conditions such as volcanoes. One alternate solution is to focus resolution on some spots of interest and to adapt the source and receiver

configuration for this purpose. In the present study, we investigate the “Puy des Goules”, a one by one kilometer conical shaped Strombolian type volcano that erupted about 10 ky ago in the *Chaîne des Puys* volcanic chain located in central France [*Goër*, 2001] (Figure 1). Our objective is to determine the structure of the high velocity feeding system located at the base of low density scoria cone, and right above the gneissic bedrock.

2. Data and Methods

2.1. Experimental Design and Data Processing

[3] The survey took place in November 2004 and lasted for 1 month. We used the newly designed High Resolution Imaging (HRI) array (O. Coutant et al., The High Resolution Imaging portable array, a seismic (and internet) network dedicated to seismic imaging, manuscript in preparation, 2006): 258 seismic sensors were deployed, 48 along refraction profiles and 210 within 30 clusters of 7 sensors at fixed locations (Figure 1). These locations were spaced 20 m apart and were distributed on a 3D pattern designed to maximize resolution at the cone basement. Two different seismic sources were used, a 16 ton Mertz vibrator on roads and trails (370 sites), dynamite shots off trails (2 to 6 kg, 30 sites). Source locations were distributed along four lines P1, P2, P3 and P3b for refraction profiles and homogeneously distributed around and within the receiver network for tomography. The vibrating source function was a 10 to 110 Hz linear frequency sweep. One important issue was to pick accurately the first arrival times, (a) on causal signal (explosive source) and null phase correlated signal (vibrator), (b) on emergent arrivals in area where scattering effects are very strong [*Wegler and Lühr*, 2001]. To improve picking in critical cases, we used relative picking by cross-correlating emergent arrivals on close-by stations, moving toward an impulsive master traces. We selected a total of 3600 first arrival times (approximately 60 source sites recorded at 60 sensor locations (Figure 2)) with errors smaller than 7 ms. Positioning was performed for all source and receiver locations by GPS static survey with a 1 cm accuracy. Accurate positioning is needed because a 5 m error in location can yield an error as large as 10 ms in travel times at 500 m/s, the average velocity measured at surface. The full data set was unfortunately partly reduced due to very cold weather conditions that induced malfunctioning equipment. This mostly affected the recording on the eastern part of the volcano.

2.2. Initial Velocity Model

[4] Preliminary 2-D velocity measurements were performed prior to the main experiment to prepare the sensor deployment and to help define the initial 3D velocity model. We conducted 2-D refraction and tomographic seismic profiles along the cone in two perpendicular directions.

¹Laboratoire de Géophysique Interne et Tectonophysique, Grenoble, France.

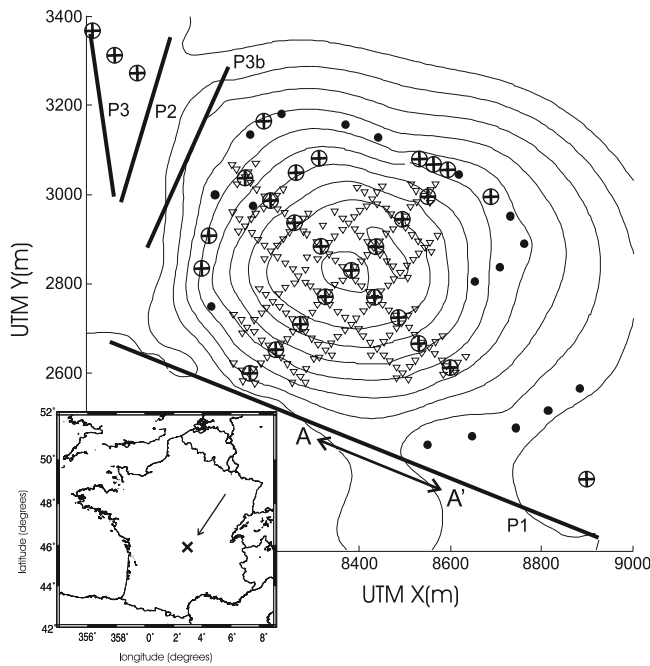


Figure 1. Puy des Goules location and field survey geometry. Triangle: geophone fixed locations; Encircled cross: explosive sources; Black thick lines and dots: vibrator shot lines and shot sites. A-A' denotes the location of the profile shown in Figure 3. Contour lines are plotted every 20 m from foot 960 m, to top 1140 m.

One seismic profile recorded along the southern flank of the cone is shown in Figure 3. It clearly shows the presence of the high velocity (≈ 4500 m/s) metamorphic bedrock beneath the scoria layer. This result was confirmed by adjusting the depth and velocity of the bedrock with a trial-and-error minimization of the travel-time residuals, using a 3D model with topography and bedrock. We found an optimal depth of 880 m and a velocity of 4500 m/s for the bedrock. Scoria P wave velocity obtained on these profiles was comprised between 500 m/s and 2000 m/s.

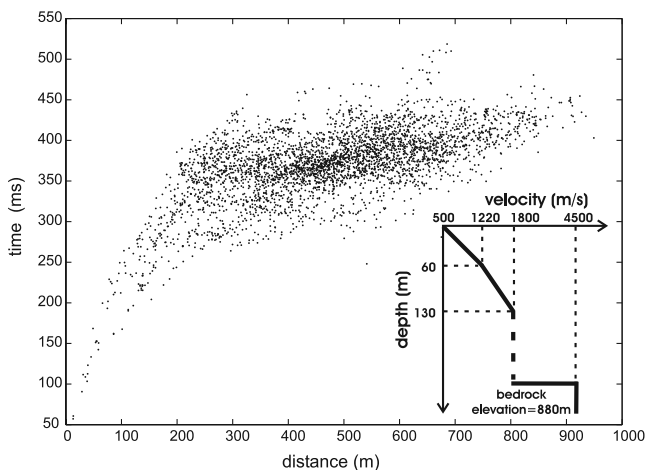


Figure 2. P wave travel times used for inversion versus horizontal shot-receiver distance along topography. Inset shows the 1D vertical P wave velocity profile used for the inversion starting model.

[5] We define the 3D initial velocity model above the bedrock with vertical velocity gradients defined with respect to the topography level. This is consistent with the building of the cone made of different layers, ash deposit, lava flows, that we assume at first to be constant around the cone. The gradients are deduced from the travel times (Figure 2) using Herglotz-Wiechert 1D formula at offsets below 300 m. The P wave velocity profile is shown in Figure 2. This initial model considers a constant velocity at surface (500 m/s) while we observed large variations, from 350 m/s to 700 m/s, in short offset data recorded across several clusters. To correct these near surface effects, we compute average residuals at source and stations and directly correct the travel time, a method similar to station corrections used in tele-seismic tomography. This approach is more suitable than inverting for near surface velocities since we focus resolution on the cone basement.

2.3. Traveltime Computation and Inversion

[6] Travel times may be difficult to compute in very heterogeneous media with strong velocity contrasts like volcanoes. *Nishi* [2001] for instance proposes a stable hybrid method based on the shortest path method. We improve the hybrid method proposed by *Latorre et al.* [2004] based on the Fast Marching Method by *Podvin and Lecomte* [1991] and a gradient based ray tracing procedure. This method allows models with complex topography. It yields the ray path coordinates, the first Fresnel zone volume and the travel times with an accuracy of a few milliseconds with a grid size of 12 m in the three directions. The full size of the model used in the study is $108 \times 102 \times 37$. For inverting travel times, we use the first Fresnel volume as in the *Fat Ray Concept* [*Husen and Kissling*, 2000] but using an algebraic Simultaneous Iterative Reconstruction Technique (SIRT) similar to *Watanabe et al.* [1999] rather than a linearization method. As shown by *Baig et al.* [2003] and *Yang and Hung* [2005], travel times computed by the ray theory in complex media are valid for velocity heterogeneities whose size are larger than half the Fresnel volume width. This defines our lateral resolution to approximately 80 m at bedrock level, given a dominant frequency of 25 Hz.

[7] We back-projected travel time residuals on the first Fresnel volume computed in the 3D velocity model of the previous iteration. Despite its simplicity, SIRT method is

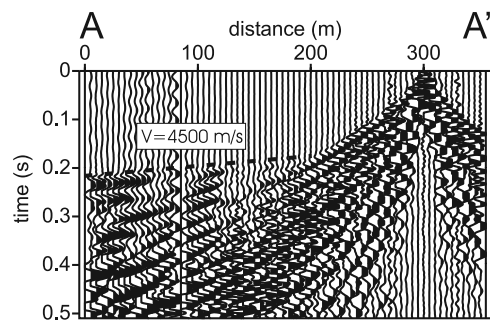


Figure 3. Seismic profile operated with the vibrator along the southern flank of the volcano. See A-A' positions in Figure 1. The velocity V is the apparent velocity of the P refracted waves on the metamorphic bedrock.

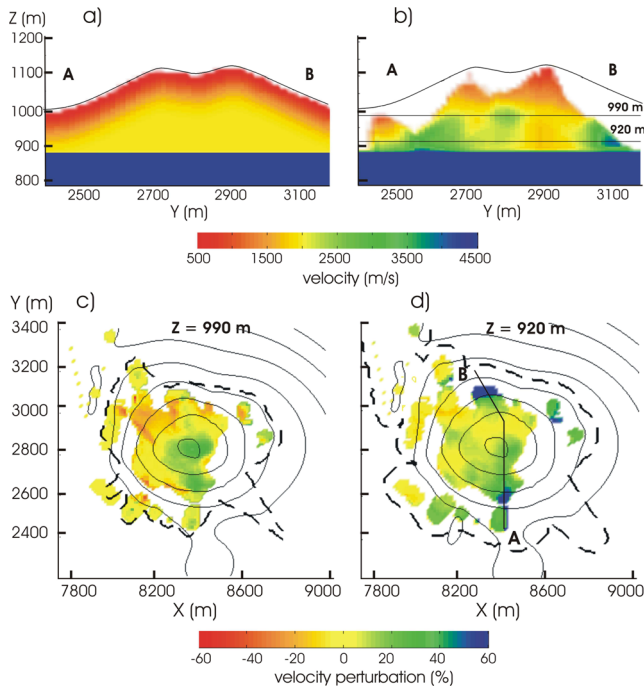


Figure 4. Travel-time inversion results. (top) Vertical cross-sections along profile AB: (a) initial P wave velocity model and (b) absolute velocity after inversion. (bottom) Horizontal cross-section at (c) 990 m and (d) 920 m with relative variations $(V_{\text{final}} - V_{\text{start}}) / V_{\text{start}}$. Dashed lines show the limit of the inverted area. Continuous lines show topography contour lines every 40 m. Areas with less than 40 Fresnel zone contributions are not shown.

known to converge toward the least-square solution [Trampert and Levêque, 1990]. In our case, it is an easy way to implement an inversion procedure based on the ray method described above, that satisfies the ray theory validity conditions and that allows to keep parts of the velocity model fixed during inversion.

[8] An important local geological feature of the *Chaîne des Puys* volcanism, is the presence of a metamorphic bedrock at shallow depth below scoria or lava flow layers. We will assume in our travel time inversion that this metamorphic basement does not show large velocity and topography fluctuations below the “Puy des Goules” and we keep its velocity fixed during inversion. It seems reasonable to neglect bedrock velocity perturbations smaller than 10 percent compared to the large velocity perturbations expected inside the cone. The topography smoothness is more questionable, but our ray coverage does not allow to solve for it. It is however consistent with close-by outcrop observations (1.5 km East and 5 km West [Goër et al., 1991]) and our local refraction profiles performed east of the cone along profile P2 (not shown) and P3b (Figure 3). Finally, drill log results available from 20 to 25 m deep boreholes drilled 1 km east of the volcano (courtesy of P. Labazuy, OPGC) show homogeneous scoria filling down to 25 m depth. We show in Figure 4 the tomography results. The RMS on time residuals decreases from 30 ms to 9 ms. Three slices are shown, above the bedrock at 920 m and 990 m, and a vertical slice crossing the three major high velocity perturbations. Several starting models were tried with different values of gradient that affect

the initial velocity at the center. For all of these models, we retrieve the central high velocity anomaly. We also inverted the travel times, with or without surface velocity corrections. Again, this does not affect the global image, but it changes the absolute velocity values of the major heterogeneities. One major limitation of algebraic reconstruction techniques is that they do not yield a direct estimate of the resolution. Instead, we use two different ways to assess the validity of our results. First, we compute the ray coverage and keep only the velocity estimates for which we observe more than 40 Fresnel zones contributions. Second, we perform a spike test. The synthetic first arrival times are calculated in the initial velocity model completed by three $80 \text{ m} \times 80 \text{ m} \times 80 \text{ m}$ boxes of high velocity ($V = 4500 \text{ m/s}$) at locations corresponding to the three imaged major high velocity anomalies (Figure 5a). We then invert these synthetic data in the same manner as for the real data (Figures 5b, 5c, and 5d). We prefer to perform spike tests rather than checkerboard tests because we invert for high velocity perturbations (more than 60%) that strongly affect ray geometries and because we concentrate the resolution on a small region rather than the full volume usually spanned by the checkerboard geometry. Figure 5 shows that only two of the three heterogeneities are recovered. The third one, located south of the cone is very close to a poor ray coverage area and does not show as clearly as in Figure 4.

3. Discussion

[9] The central and the northern high velocity heterogeneities ($V \approx 4000 \text{ m/s}$) are the most stable features that

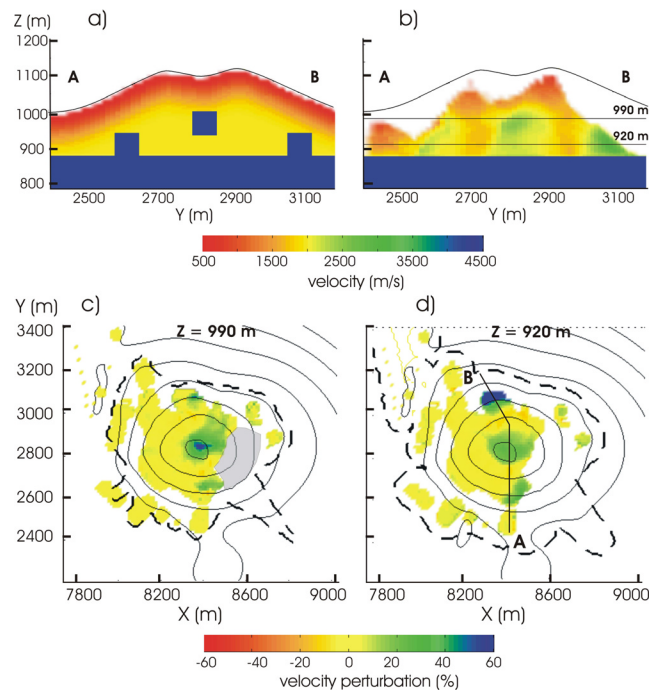


Figure 5. Spike test results. (top) Vertical cross-sections along profile AB: (a) spike velocity model used for test and (b) absolute velocity after inversion. (bottom) Horizontal cross-sections at (c) 990m and (d) 920 m with relative variations $(V_{\text{final}} - V_{\text{start}}) / V_{\text{start}}$. Same dash and continuous lines legends as for Figure 4. Gray zone displays the poorly resolved area due to data loss.

could be recovered from the data and validated by the spike test. The northern heterogeneity can be interpreted as intrusive trachytic rocks such as feeder conduits or dike source that extend at the cone basement. Its shape looks similar to that observed on the nearby “Puy de Lemptégy”, and the velocity is close to our laboratory ultrasonic measurements (4500 m/s) performed on Lemptégy’ Trachyte samples. The lateral extent is about the size of the lateral resolution that we can expect with our configuration (80 m). The high velocity at center can be interpreted as dense material that forms the main chimney. Its vertical extension is poorly resolved since the associated localized spike is recovered with a longer height, but its lateral extension seems to be smaller than the 80 m width spike. The southern high velocity heterogeneity cannot be interpreted as the northern one since it clearly lacks resolution despite some correlation with the cone topography. These results are in agreement with our hypothesis of a smooth bedrock geometry. The areas with high velocity perturbation have small lateral extension in zones with good ray coverage. Keeping the bedrock fixed during the inversion is also consistent with our results: the SIRT method is based on the approximate equality $dT/T \approx dS/S$ along rays (T travel time, S slowness) and the high velocity perturbations found above the bedrock (>60%) would be equally present below, leading to unrealistic velocity values (7500 m/s observed when inverting bedrock). Our objective was to study the small scale structure of a Strombolian volcano by focusing the resolution on a limited area, the cone basement, in order to reach the finest resolution. We demonstrate the validity of this focused resolution approach including a pre-step of survey planning necessary to optimize the acquisition geometry. Moreover, we reach a resolution as good as usual volcanic tomography (80 m/1000 m compared to 1 km/10 km) on a smaller scale of investigation. This is the first preliminary step toward finer resolution. Aside from the limitation due to the travel time inversion approach, we see several ways to increase the resolution using similar data set: improving the travel time computation accuracy that is currently of a few millisecond compared to the 9 ms RMS after inversion, using waveform modelling to compute finite frequency travel time and kernel [Nolet et al., 2006] and using shear waves travel times. This last point is crucial in geological context like volcanic areas where material properties can exhibit strong differences between P and S waves. This problem can be addressed by using natural seismic sources or vibrators. An interesting observation is that vibrators using either vertical or transverse surface excitation generate both P and S waves, according to vertical or horizontal force radiation diagram. Some vibrator S waves for instance were clearly recorded at some sites and could be processed and inverted in a next study.

[10] **Acknowledgments.** This work was supported by the “Natural hazards mitigation” program of the French Ministry of Research. We thank

all the people who participated to the experiment and E. Chaljub (LGIT), F. Guyoton (Géolithe SARL), P. Labazuy (OPGC), I. Lecomte (NORSAR), J. Mars (LIS), and J. Virieux (U.Nice) for their help; the Dômes Union association for giving us access to the field; and V. Monteiller for inversion comparisons with LSQR method. Comments by J. R. Grasso and two anonymous reviewers improved the manuscript significantly.

References

- Baig, A. M., F. A. Dahlen, and S.-H. Hung (2003), Traveltimes of waves in three-dimensional random media, *Geophys. J. Int.*, *153*, 467–482.
- Goër, A. (2001), Les volcans du Massif central, *Geologues*, *3947*(130–131), 66–91.
- Goër, A., G. Camus, P. Boivin, A. Gourgaud, G. Kieffer, J. Mergoïl, and P.-M. Vincent (1991), Carte géologique de la chaîne des Puys, in *Volcanologie de la Chaîne des Puys*, edited by L. Galtier, Parc Nat. Reg. des Volcans d’Auvergne, Aydat, France.
- Husen, S., and E. Kissling (2000), Local earthquake tomography between rays and waves: Fat ray tomography, *Phys. Earth Planet. Inter.*, *3947*, 1–21.
- Kodaira, S., K. Uehira, T. Tsuru, H. Sugioka, K. Suyehiro, and Y. Kaneda (2002), Seismic image and its implications for an earthquake swarm at an active volcanic region off the Miyake-jima–Kozu-shima, Japan, *Geophys. Res. Lett.*, *29*(11), 1548, doi:10.1029/2001GL014377.
- Laigle, M., A. Hirn, M. Sapin, J. C. Lépine, J. Diaz, J. Gallart, and R. Nicolich (2000), Mount Etna dense array local earthquake P and S tomography and implications for volcanic plumbing, *J. Geophys. Res.*, *105*(B9), 21,633–21,646.
- Latorre, D., J. Virieux, T. Monfret, V. Monteiller, T. Vanorio, J.-L. Got, and H. Lyon-Caen (2004), A new seismic tomography of Aigion area (Gulf of Corinth, Greece) from the 1991 data set, *Geophys. J. Int.*, *159*, 1013–1031.
- Nishi, K. (2001), A three dimensional robust seismic ray tracer for volcanic regions, *Earth Planets Space*, *53*, 101–109.
- Nolet, G., F. A. Dahlen, and R. Montelli, (2006), Traveltimes and amplitudes of seismic waves: A re-assessment, in *Seismic Earth: Array Analysis of Broadband Seismograms*, *Geophys. Monogr. Ser.*, vol. 157, edited by A. Levander and G. Nolet, pp. 37–47, AGU, Washington, D. C.
- Podvin, P., and I. Lecomte (1991), Finite difference computation of travel times in very contrasted velocity models: A massively parallel approach and its associated tools, *Geophys. J. Int.*, *105*, 271–284.
- Scarpa, R., F. Tronca, F. Bianco, and E. D. Pezzo (2002), High resolution velocity structure beneath Mount Vesuvius from seismic array data, *Geophys. Res. Lett.*, *29*(21), 2040, doi:10.1029/2002GL015576.
- Tanaka, S., et al. (2002), Three-dimensional P-wave velocity structure of Iwate volcano, Japan from active seismic survey, *Geophys. Res. Lett.*, *29*(10), 1420, doi:10.1029/2002GL014983.
- Trampert, J., and J.-J. Levêque (1990), Simultaneous iterative reconstruction technique: Physical interpretation based on the generalized least squares solution, *J. Geophys. Res.*, *95*(B8), 12,553–12,559.
- Watanabe, T., T. Matsuoka, and Y. Ashida (1999), Seismic traveltime tomography using Fresnel volume approach, *SEG Expanded Abstr.*, *18*, 1402.
- Wegler, U., and B.-G. Lühr (2001), Scattering behaviour at Merapi volcano (Java) revealed from an active seismic experiment, *Geophys. J. Int.*, *145*, 579–592.
- Yamawaki, T., et al. (2004), Three-dimensional P-wave velocity structure of Bandai volcano in northeastern Japan inferred from active seismic survey, *J. Volcanol. Geotherm. Res.*, *138*, 267–282.
- Yang, H.-Y., and S.-H. Hung (2005), Validation of ray and wave theoretical travel times in heterogeneous random media, *Geophys. Res. Lett.*, *32*, L20302, doi:10.1029/2005GL023501.
- Zollo, A., L. D’Auria, R. D. Matteis, A. Herrero, J. Virieux, and P. Gasparini (2002), Bayesian estimation of 2-D P-velocity models from active seismic arrival time data: Imaging of the shallow structure of Mt Vesuvius, *Geophys. J. Int.*, *151*, 566–582.

H. Baudon, F. Brenguier, O. Coutant, M. Dietrich, and F. Doré, LGIT, BP 53, F-38041 Grenoble Cedex 9, France. (olivier.coutant@ujf-grenoble.fr)